Advances in Water Resources 33 (2010) 1268–1278

Contents lists available at ScienceDirect

Advances in Water Resources

journal homepage: www.elsevier.com/ locate/advwatres

Numerical modeling of the effects of water flow, sediment transport and vegetation growth on the spatiotemporal patterning of the ridge and slough landscape of the Everglades wetland

Marcelo E. Lago [a], Fernando Miralles-Wilhelm [b,*], Mehrnoosh Mahmoudi [b], Vic Engel [c]

[a] DHI Water and Environment, Inc., Tampa FL, USA
[b] Dept. of Civil and Environmental Engineering, Florida International University, Miami FL, USA
[c] National Park Service, South Florida Ecosystem Office, Homestead, FL, USA

ARTICLE INFO

Article history:
Received 14 October 2009
Received in revised form 17 July 2010
Accepted 29 July 2010
Available online 6 August 2010

Keywords:
Modeling
Ridge and slough
Patterning
Everglades

ABSTRACT

A numerical model has been developed to simulate the spatiotemporal patterning of the ridge and slough landscape in wetlands, characterized by crests (ridges) and valleys (sloughs) that are elongated parallel to the direction of water flow. The model formulation consists of governing equations for integrated surface water and groundwater flow, sediment transport, and soil accretion, as well as litter production by vegetation growth. The model simulations show how the spatial pattern self-organizes over time with the generation of ridges and sloughs through sediment deposition and erosion driven by the water flow field. The spatial and temporal distributions of the water depth, flow rates and sediment transport processes are caused by differential flow due to vegetation and topography heterogeneities. The model was parameterized with values that are representative of the Everglades wetland in the southern portion of the Florida peninsula in the USA. Model simulation sensitivity was tested with respect to numerical grid size, lateral vegetation growth and the rate of litter production. The characteristic wavelengths of the pattern in the directions along and perpendicular to flow that are simulated with this model develop over time into ridge and slough shapes that resemble field observations. Also, the simulated elevation differences between the ridges and sloughs are of the same order of those typically found in the field. The width of ridges and sloughs was found to be controlled by a lateral vegetation growth distance parameter in a simplified formulation of vegetation growth, which complements earlier modeling results in which a differential peat accretion mechanism alone did not reproduce observations of ridge and slough lateral wavelengths. The results of this work suggest that ridge and slough patterning occurs as a result of vegetation's ability to grow laterally, enhancing sediment deposition in ridge areas, balanced by increased sediment erosion in slough areas to satisfy flow continuity. The interplay between sediment transport, water flow and vegetation and soil dynamic processes needs to be explored further through detailed field experiments, using a model formulation such as the one developed in this work to guide data collection and interpretation. This should be one of the focus areas of future investigations of pattern formation and stability in ridge and slough areas.

1. Introduction

The formation, vulnerability and resilience of spatiotemporal patterns in water-controlled ecosystems have been tied to phenomena that link the cycling of water, sediments, nutrients and other biogeochemically active elements. Understanding the perturbations in these cycles that trigger impacts on ecosystem spatiotemporal characteristics is a challenge that generally transcends disciplinary and geographical boundaries, and is key to sustaining the diversity of life on Earth. Water-controlled ecosystems are those in which either excess and/or deficit of water and nutrients are determinants of its structure and function, have complex dynamic characteristics that depend on many interrelated links between climate, soil, water and nutrient availability, and vegetation. For instance, climate and soil have a key influence on patterns of vegetation distribution [24,26]; in turn, vegetation physiological processes condition the water and nutrient balances of the ecosystem [21,23,33]. Wetlands are major representatives of such water-controlled ecosystems.

Wetlands throughout the world commonly show various spatial patterning of hummocks and hollows [2,20,29]. Particularly, low-elevation gradient wetlands exhibit spatial patterning in vegetation distribution exhibited by formations parallel (longitudinal) or perpendicular to the flow, such as *string patterns* [11] consisting of regular densely vegetated bands (crests forming ridges), alternating

* Corresponding author.
E-mail address: miralles@fiu.edu (F. Miralles-Wilhelm).

0309-1708/$ – see front matter © 2010 Elsevier Ltd. All rights reserved.
doi:10.1016/j.advwatres.2010.07.009

with lower/wetter zones that are more sparsely vegetated (valleys forming sloughs). Examples of wetlands with longitudinal patterning include tree islands [1,10] and ridge and slough landscape of the Florida Everglades [18,22], the Okavango Delta [9,12], the llanos in Venezuela and Colombia [30], the Brazilian Pantanal [32], and the Sian Ka'an coastal wetlands in the Yucatan peninsula [25]. In these wetlands, islands or ridges with trees or herbaceous vegetation are interspersed among open-water conduits aligned parallel to the regional flow direction.

Several theoretical and empirical investigations have shown that such spatial patterning in wetlands can be explained by a positive feedback mechanism between plant productivity and flow and transport processes [27,34]. Thus, a wetland surface with slight initial differences between more densely vegetated, drier sites and wetter, more sparsely vegetated areas, may further differentiate and develop spatial patterning over time. Ecohydrological models have provided tools to test hypotheses about feedback and self-organization mechanisms and compare against observed landscape characteristics [13,14,27,36]. Models have also upheld the hypothesis that development of perpendicular-to-slope string patterning in wetlands occurs in a stability space defined by crest-to-valley hydraulic conductivity ratios and regional slope, in which lower hydraulic conductivity ratios and steeper slopes favor pattern development [3,4,27,34]. However, application of ecohydrological modeling to elucidate landscape patterns and processes in longitudinally patterned wetlands has been much less common [17,18]. Here, mechanisms for creating and maintaining environmental heterogeneity are complex, involving feedback between physical and biological processes including peat and organic matter production and redistribution of material and nutrients through flow and transport processes. To better understand the dominant ecological feedbacks controlling the landscape dynamics in these patterned wetlands, new theories and testable ecohydrological models are needed.

In this investigation, focus is placed on modeling the feedback between water flow, sediment transport (erosion and deposition), vegetative litter production and decomposition, and dynamic soil accretion. A numerical model of proposed governing equations for these processes is developed and applied to the ridge and slough landscape using parameters for the Everglades wetland. This model is used to explore the hypothesis of whether observed landscape features and long term stability of the ridge and slough landscape can be explained through the interaction of these coupled processes. This investigation complements the work by Larsen et al. [18], who hypothesized the importance of sediment transport in the ridge–slough pattern formation. Results and insight gained from the conceptual and numerical models provide an improved mechanistic understanding of how the landscape may have formed and developed over time. This effort is a step further towards a framework for future modeling and data collection research intended to improve management and decision making in ecosystem restoration efforts.

2. Study area

The Everglades are a subtropical wetland located in the southern portion of Florida. The system begins near Orlando with the Kissimmee River, which discharges to the Lake Okeechobee in the north and ends at Florida Bay in the south. The Everglades are also referred to as the *river of grass* [8], referring to the sawgrass marshes covering a large portion of this ecosystem. The ridge and slough system in the Everglades is found commonly in the center and southern portion of the wetland, as depicted in Fig. 1.

Ridges in the Everglades are found as elevated elongated topographic features covered by vegetation such as sawgrass (*Cladium jamaicense*). It has been hypothesized that peat deposition extends the ridge while water flow transports sediments and decreases the ridge extension by erosion. Sloughs, or free-flowing

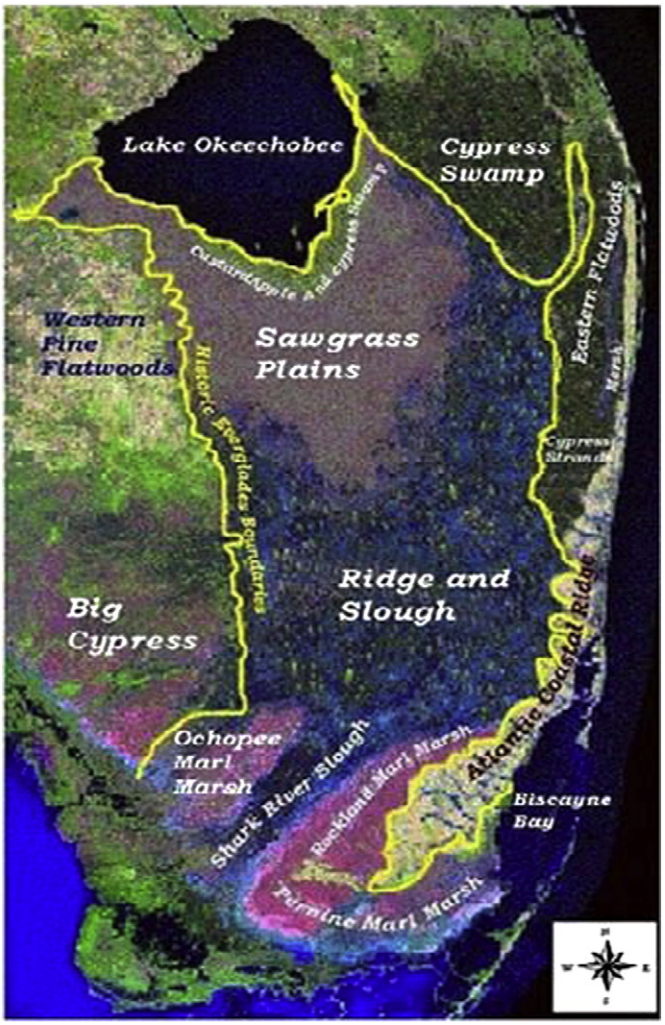

Fig. 1. The Everglades wetland located within the southern Florida peninsula (Source: http://edis.ifas.ufl.edu).

channels of water, develop in between sawgrass ridges. In the Everglades, sloughs are typically on the order of 1 m deeper than sawgrass marshes, and may stay flooded most of the time. The spatial average of ground surface elevations in the study area is approximately 1.4 m NGVD; a slight elevation gradient of less than 5 cm/km from Lake Okeechobee to Florida Bay results in a slow flowing system with Reynolds numbers $Re \approx O(100–1000)$ based on water depth and flow velocity [17].

The ridge and slough landscape in the Everglades has been slowly degraded over the past century. This degradation is evidenced as a loss of sloughs and their connectivity in areas of the Everglades that have been exposed to changes in hydrology driven by water management practices (see Fig. 2), as well as the expansion of sawgrass to dry areas created by the same practices. Studies of the ridge and slough landscape throughout the Everglades (e.g., [5,22,31]) document how these communities are reacting to new hydrological regimes. Field surveys suggest that present vegetation communities are out of equilibrium with local hydrology. Loss of ridge and slough landscape has been defined by the regional Science Coordination Team [31] as a loss of elevation difference between ridge height and slough depths resulting in a flattening of the landscape and a loss of distinct ridge and slough vegetation growth aligning with flow direction.

Nevertheless, ridge and slough development and maintenance mechanisms remain to be fully understood and documented. Loss of peat soils may help to flatten the ridge and slough landscape. A

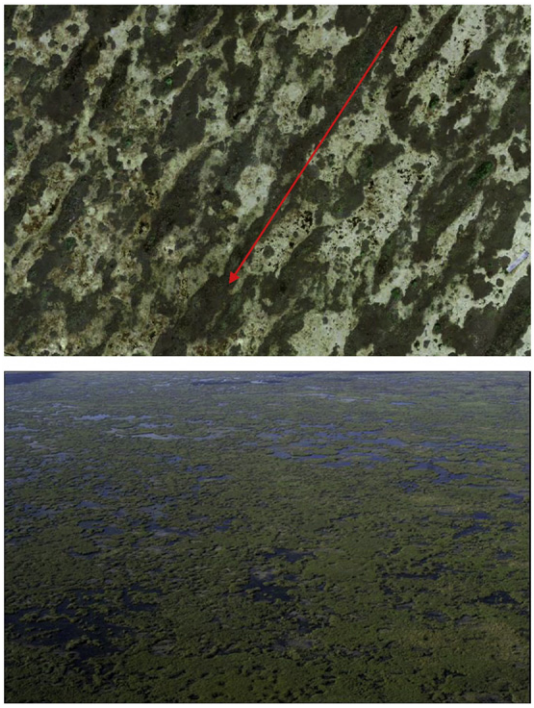

Fig. 2. Examples of preserved (above) and degraded (below) ridge and slough. Sources: above, Google Earth view of ridge–slough patterns in Shark Slough Valley around coordinates 25°38′39.47″N, 80°43′51.12″W. The sheet flow direction is highlighted with a red arrow; below, http://edis.ifas.ufl.edu).

shortening in the wetland's hydroperiod and low groundwater levels can increase loss rates of peat soils since oxidation of the top peat layers of ridge and slough occurs in drier areas. Each vegetation species can survive within specific ranges of water depths and quality. Therefore, when water levels and hydroperiods are manipulated for water management objectives, vegetation will respond differently and their composition and growth will change. Different rates of vegetation decay may also change the ridge and slough landscape. Research has shown that plants that grow in sloughs, such as fragrant water lily (*Nymphaea odorata*), decompose much faster than plants that grow on ridges, such as sawgrass [6]. When comparing field litter, 60% of sawgrass remained after a year, while slough species decayed within a few months. These decay rate differences could help maintain differences between ridges and sloughs elevation. Decreases in flow also can create stationary conditions which results in reduction of dissolved oxygen concentrations in sloughs, slowing down decomposition rates, but causing in faster peat accumulation and eventual filling in of sloughs.

3. Conceptual model

The coupled spatial and temporal dynamics of water flow and sediment transport are conceptualized as follows (and depicted in Fig. 3):

(1) The conceptual model has two vertical layers: surface water (overland) and soil. These layers have water pools that are communicated horizontally (x,y) and vertically (z).
(2) Particulate sediment pools occur in the surface water and soil layers; these pools are composed by inorganic and organic particles. Organic particles are produced by vegetation (as litter) and deposited in surface water (above ground production), and in soil (below ground or root production).

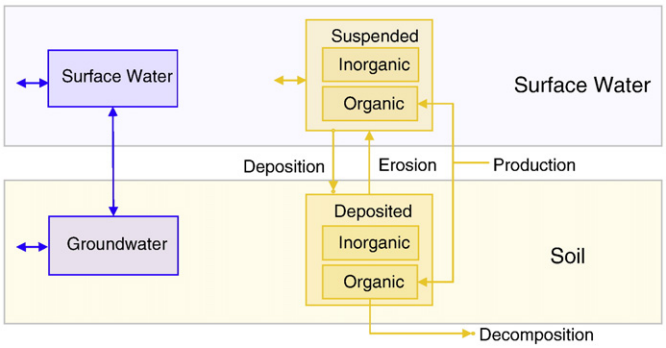

Fig. 3. Proposed conceptual model for water flow and sediment transport mechanisms in the ridge and slough landscape.

(3) The suspended particles can flow laterally in the surface water layer due to convective and dispersive transport. The vertical fluxes of particles between the two layers are due to deposition and erosion processes.
(4) Deposited organic particle mass in the soil pool is removed by decomposition.

The effect of each biophysical phenomenon in ridge and slough pattern formation is summarized in Table 1.

4. Governing equations

4.1. Surface water flow

The overland flow of water is formulated through the vertically averaged continuity (conservation of mass) and momentum equations. The continuity equation is written as:

$$\frac{\partial h}{\partial t} + \frac{\partial}{\partial x}(hV_x) + \frac{\partial}{\partial y}\left(hV_y\right) = -\varepsilon_{GW}, \tag{1}$$

where h [L] is the surface water depth (above the ground), V_x [LT^{-1}] and V_y [LT^{-1}] are the horizontal velocity vector components. Recharge to groundwater ε_{GW} [LT^{-1}] is written in a simplified Darcian form, driven by the head difference between surface water and groundwater:

$$\varepsilon_{GW} = \frac{K}{\delta}(h + z_b - H). \tag{2}$$

Here, K [LT^{-1}] is the hydraulic conductivity of the surface soil through which recharge occurs, δ is the vertical distance over which the head difference $(h + z_b - H)$ is measured. In this model, δ is numerically approximated as half the depth of the groundwater modeling cells. H [L] is the elevation of the groundwater table above the datum. The topography z_b [L] is the ground surface elevation above the datum.

Other water sources and sinks (rainfall and evaporation) are not considered directly in the continuity equation; their regional effect in the water table level is considered through the boundary conditions as explained below.

For conservation of momentum, a diffusive-wave approximation is implemented in the model formulation. This approximation is valid for the typical slow flow, i.e., small Reynolds number conditions encountered in the Everglades wetland [15,16,37]. In particular, the Manning's equation is utilized for the absolute horizontal velocity:

$$V = \frac{1}{n}h^{\frac{2}{3}}S^{\frac{1}{2}}, \text{ and} \tag{3}$$

Table 1
Biophysical phenomena and their expected effects on ridge and slough patterning.

Phenomenon	Depends on	Effect on ridge and slough	Expected pattern effect
Vegetation biomass production rate	–Type of vegetation –Water table level (oxygen stressed)	More production in ridges covered by sawgrass	Making elevation higher in vegetated ridges
Vegetation mass decomposition rate	–Water table level (aerobic or anaerobic) –Depth and organic fraction in soil	More decomposition in higher elevated ridges with thicker organic soils	Limiting the soil elevation in ridges
Net erosion (erosion–deposition)	–Water velocity field, i.e., local bed resistance and water depth but also on their spatial distribution –Suspended particle concentration	Lower water speed (erosion) in the front and in the rear of flow obstacles (ridges) and higher at the sides Higher deposition in front and rear, where particles are transported from sites with higher speed	Elongating ridges and making lateral sloughs deeper
Biomass lateral growth	–Differences in vegetation coverage	More vegetation and therefore, more production and bed resistance in ridges vegetated edges	Thickening of ridges

$$V_j = -V\frac{S_j}{S}, S_j = \frac{\partial(z_b + h)}{\partial j}, j = x, y. \tag{4}$$

Here, n is the Manning coefficient representing resistance to surface flow, which in the case of flow over vegetated wetlands, n can be interpreted as characterizing the relative roughness of the vegetation, e.g., a lower n corresponds to lesser resistance to flow (e.g., marsh grass surface), while a higher n would correspond to denser vegetation (e.g., trees). S_x and S_y are the components of the surface slope with absolute value S; all slopes are non-dimensional.

4.2. Groundwater flow

The continuity equation averaged in an unsaturated porous space is written as:

$$\frac{\partial}{\partial t}(\phi S_w) + \frac{\partial V_x}{\partial x} + \frac{\partial V_y}{\partial y} + \frac{\partial V_z}{\partial z} = 0, \tag{5}$$

where S_w (non-dimensional) is the water saturation, V [LT^{-1}] is the macroscopic velocity vector and ϕ (non-dimensional) is the soil porosity.

The momentum equation for groundwater takes the form of Darcy's equation, with the following expression for the velocity components in three directions:

$$V_j = -Kk_r\frac{\partial H}{\partial j}, j = x, y, z. \tag{6}$$

Here, k_r (non-dimensional) is the relative permeability. The Brooks and Corey correlation is used for the relative permeability, and the Van Genuchten correlation [35] is used for the moisture retention curve that relates pressure head and saturation, so that:

$$k_r = S_w^m \tag{7}$$

$$S_w = \begin{cases} \left[1 + |\alpha\psi|^{\beta}\right]^{-\gamma} & \text{for } \psi<0 \\ 1 & \text{for } \psi\geq 0 \end{cases}, \psi = H - z, \gamma = 1 - \frac{1}{\beta}. \tag{8}$$

Here m is the Brook–Corey exponent, $-\psi$ [L] is the capillary pressure head and α [L^{-1}], β and γ are the Van Genuchten parameters; m, β and γ are non-dimensional.

4.3. Balance equation for suspended particles

Two balance equations for the suspended particles (inorganic and organic) in overland water flow are found by considering advection-dominated transport and corresponding source/sink terms. The advection-dominated assumption is justified based on estimated Peclet numbers for the transport regime larger than Reynolds numbers for the flow regime, i.e., Pe>O(100–1000), given that the ratio of viscosity to diffusion/dispersion coefficients (Sc>1) for water, and Pe = Re Sc.

The transport equations for the suspended particles can then be written as:

$$\frac{\partial}{\partial t}\left(hC_j\right) + \frac{\partial}{\partial x}\left(hV_xC_j\right) + \frac{\partial}{\partial y}\left(hV_yC_j\right) = \varepsilon_{prod,j} - \varepsilon_{dep,j} + \varepsilon_{ero,j}. \tag{9}$$

Here, C_j [ML^{-3}] is the suspended particles concentration, $j = O$ for organic and $j = I$ for inorganic, ε_{prod} [$ML^{-2}T^{-1}$] is the above ground litter production rate, ε_{dep} [$ML^{-2}T^{-1}$] is the deposition rate and ε_{ero} [$ML^{-2}T^{-1}$] is the erosion rate. Production of sediment organic particles (e.g., litter from vegetation) is assumed to occur above ground (e.g., falling leaves) and below the ground (e.g., root debris). The production rate of inorganic particles is assumed negligible.

The particle deposition and erosion rates are formulated through the relations:

$$\varepsilon_{dep,j} = v_SC_j; \varepsilon_{ero,j} = f_j\left(\varepsilon_{res} + F_E\left(\frac{V}{v_S}\right)^2\right). \tag{10}$$

Here, v_S is the settling (Stokes) velocity, f_j is the mass fraction of particle types in soil, ε_{res} is the resuspension rate and F_E is a proportionality parameter controlling increasing erosion with water velocity [17,19]. The resuspension rate is included on Eq. (10) in order to take into account processes (other than erosion) that contribute to the resuspension of the particles. In the case of the Everglades, the rewetting of dry areas can resuspend dry litter (with a lower bulk density than water) [38]; the production of gas in the peat layer can also produce particle resuspension, as well as near-bottom processes such as wind waves, animal activity, and others.

4.4. Soil balance equation

The mass balance equations for the deposited organic and inorganic particles are given by the following dynamic relations:

$$\frac{\partial L_O}{\partial t} = f_{BA}\varepsilon_{prod,O} - r_{dec}L_O + f_O\left(\varepsilon_{dep,O} - \varepsilon_{ero,O}\right), \tag{11}$$

$$\frac{\partial L_I}{\partial t} = f_I\left(\varepsilon_{dep,I} - \varepsilon_{ero,I}\right), \tag{12}$$

where L_O [ML^{-2}] and L_I [ML^{-2}] are the mass of deposited particles per unit area. The decomposition rate r_{dec} is assumed to be aerobic for the zone above the water table; below the water table, the decomposition is assumed to occur anaerobically [7]. f_{BA} is the ratio of below ground to above ground production rate.

The dynamics of soil accretion z_b is given by the combined rate of change of deposited particles:

$$\frac{\partial z_b}{\partial t} = \frac{\partial}{\partial t}\left[\frac{L_O}{\rho_O} + \frac{L_I}{\rho_I}\right] \tag{13}$$

where ρ_O and ρ_I are the bulk densities of organic and inorganic particles, respectively.

4.5. Vegetation growth equations

In this formulation, vegetation growth is modeled in a heuristic fashion: an increase in topography due to soil accretion may reduce the oxygen stress in the vegetation, causing eventually an increase in the existing vegetation biomass and the succession to more productive species. This consequently has two effects. First, it increases the litter production rate (ε_{prod}) and second it increases the resistance to surface water flow (i.e., Manning's n coefficient), decreasing the flow velocity and thus increasing the rate of particle deposition. Both of these mechanisms result in a positive feedback for ridge growth (or conversely, for slough growth in case of a decrease in topography). For instance, ridge areas in the Everglades wetland are typically covered by dense sawgrass. At lower soil elevations, sawgrass becomes water (oxygen) stressed and these low-elevation areas are typically occupied by less-productive vegetation (sparse sawgrass *Eleocharis* spp. or *Nymphaea* spp.). This distribution of the vegetation according to soil elevation causes the rate of litter production and the flow resistance to increase as the soil accretion increases [18]. For the purpose of numerical calculations in this model, simple linear relationships have been used to link the rate of litter production ε_{prod} and the Manning's resistance coefficient n to the thickness of the soil (peat) layer. These relationships are illustrated in Fig. 4.

The vegetation (e.g., sawgrass) in ridge areas extends laterally and thus occupies the border of areas with lower soil elevation. This lateral growth of the vegetation introduces more production and a higher resistance to flow close to denser vegetated areas. In this model, this spatial correlation is introduced by defining a lateral vegetation growth distance parameter (d_{LG}). Thus, the litter production computed at each model cell i from the ground surface elevation according to Fig. 4 is corrected by considering the lateral vegetation growth from neighbor cells j as follows:

$$\varepsilon^*_{prod_i} = \varepsilon_{prod_i} + \sum_j \frac{d_{LG}}{\Delta X_i}\left(\varepsilon_{prod_j} - \varepsilon_{prod_i}\right)\Theta\left(\varepsilon_{prod_j} - \varepsilon_{prod_i}\right). \tag{14}$$

Here ε^*_{prod} is the litter production rate corrected for lateral vegetation growth, ΔX_i is the cell i width in the i–j direction, and Θ is the stepwise (Heaviside) function. Notice that the correction only applies if the neighbor cell j has a higher production rate than the cell of interest i. For consistency with the lateral vegetation growth process, the corrected production is restricted by the condition:

$$\varepsilon^*_{prod_i} \le Max\left(\varepsilon_{prod_i}, \varepsilon_{prod_j}\right) \quad \text{for all } j. \tag{15}$$

The corrected flow resistance (corrected Manning's coefficient) is obtained in a similar way.

$$n^*_i = n_i + \sum_j \frac{d_{LG}}{\Delta X_i}\left(n_j - n_i\right)\Theta\left(n_j - n_i\right) \tag{16}$$

with:

$$n^*_i \le Max\left(n_i, n_j\right) \quad \text{for all } j. \tag{17}$$

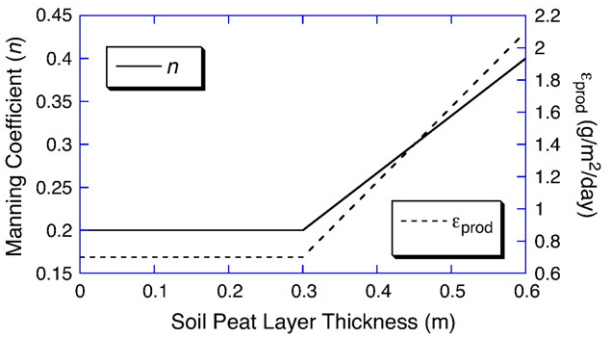

Fig. 4. Relationship between gross accretion rate (ε_{prod}) and Manning's surface resistance coefficient (n) with topography (z_b). Minimum and maximum values of ε_{prod} and n are given in Table 2. Vertical axes scale is the thickness of the soil (peat) layer, which changes due to accretion.

4.6. Boundary and initial conditions

A time-varying head boundary condition is applied at the boundaries for the hydraulic head. This time series head was obtained from historical data available for the Gumbo Limbo tree island for the period 1956–2000. The historical data was processed to find the water elevations and the regional surface water slopes for each day of the year [17]. Then, the obtained one-year time series was extended periodically through the whole simulation period.

The boundary conditions for the transport of suspended sediments are assumed as a constant concentration found assuming steady state, i.e., $(\varepsilon_{prod_j} - \varepsilon_{dep_j} + \varepsilon_{ero_j} = 0)$ at each boundary cell in the model. The deposited litter amount is assumed to be periodic in space, so that the soil depth is assumed equal in the inlet to that in the outlet boundary. In this sense, the model can be seen as a piece of a mosaic pattern extending in all directions.

The initial condition of soil surface elevation z_b is given by adding a random noise of +/−1 cm on top of a flat surface with mean elevation of 1.4 m, tilted with a regional slope of 4 cm/km, as shown in Fig. 5. The bottom of the soil layer is assumed to be a flat surface of bedrock with mean elevation of 1.0 m, tilted with the same slope, which gives an average initial soil layer depth of 40 cm.

4.7. Model parameters

A list of model parameters is shown in Table 2. The parameter values have been compiled from a number of literature sources, and should be regarded as representative of the different processes involved rather than either calibrated or unique values usable for predictive simulations. The conceptual understanding nature of this model development effort is reiterated here to highlight the focus of this investigation. The primary focus is to obtain an understanding of the mechanisms generating the ridge and slough pattern rather than a "predictive" modeling tool that would reproduce specific observations of soil elevations in a particular wetland.

5. Results and discussion

The model equations formulated above were solved numerically using a finite-volume technique detailed in [17]. The numerical solution is presented in terms of the spatiotemporal pattern of soil elevation $z_b(x,y,t)$. Fig. 6 shows the results obtained for a "base case" simulation. Results are shown for simulation times of 1 day (essentially initial conditions), and pattern evolving times of 15 years and 30 years. The soil depth variation sequences obtained are evidence of the development of an evolving pattern, elongated in the direction of the regional flow (y-direction) over time. In this

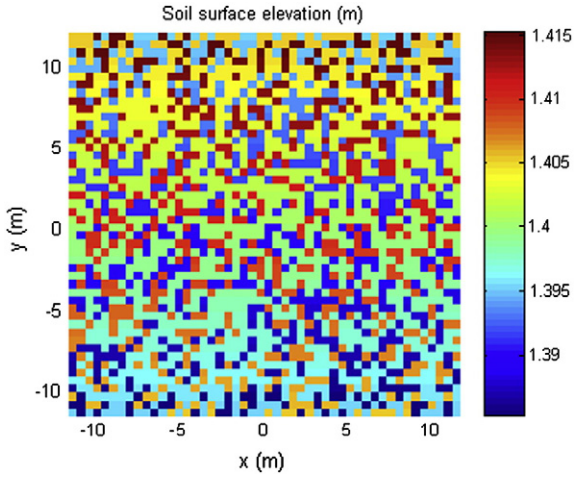

Fig. 5. Initial condition of soil surface elevation for the base case (random noise of ± 1 cm distributed spatially over a tilted flat surface with slope of 4 cm/km).

self-organizing process, the difference between the minimum and the maximum soil depths (i.e. pattern contrast) increases over time. The simulated pattern has visual similarities with the ridge and slough patterns observed in wetlands such as the Everglades. The higher and lower elevation areas in the simulated pattern will be therefore referred to as *ridges* and *sloughs*, respectively.

In order to characterize the spatial structure of the simulated ridge and slough patterns, the calculated variogram of the soil depth in the (x,y) directions is presented for each soil depth snapshot (see Fig. 7). In this representation, the pattern is revealed as a succession of maximum and minimum values in the length scale. The more organized the pattern becomes, the higher the difference between minimum and maximum values (pattern contrast). The variogram starts at a minimum value due to short range spatial correlation, i.e., close points in the landscape have similar elevations. The first maximum value in the variogram represents a typical distance between ridge and slough areas (semi-wavelength). The next minimum value corresponds to the pattern wavelength, i.e., typical distance between two ridge and two slough areas. Notice that the elongated shapes are evidence of a wavelength higher on the y (regional flow direction) than on the x (transverse) direction.

The evolution of the first maximum value (a measure of the contrast) and its position (the semi-wavelength of the pattern) are presented for the base case in Fig. 8. In the simulated period, the contrast and the wavelength are still increasing, so the pattern is still evolving. This is understandable given that the model formulation is essentially dynamic (dynamic flow field and boundary conditions). The characteristic time of pattern formation will be controlled by the flow and transport time scales embedded in the parameters used in the model simulations, particularly the production, erosion and deposition time scales in the sediment transport Eqs. (9), (11), and (12), and how these interact with the time scale of the flow field (surface and groundwater). This interplay needs to be explored through careful parameterization of the model with data specific to a given ridge and slough site. This is why it is important to carry out detailed field experiments, and use a model formulation such as the one developed in this work to guide data collection and interpretation. This should be one of the focus areas of future investigations of pattern formation and stability in ridge and slough areas.

Because of the heuristic formulation of the effect of lateral vegetation growth on litter production and flow resistance used in this work through Eqs. (14) and (16), sensitivity to the lateral vegetation growth distance d_{LG} was investigated to quantify the effect of this distance on the pattern formation. The lateral growth distance was varied from 1 m in the base case to 0, 0.25 m and 0.5 m. These results are shown in Fig. 9. When no lateral vegetation growth is considered ($d_{LG}=0$), the typical case in the x-direction is a ridge cell anteceded and preceded by a slough cell (semi-wavelength = 1 grid cell). This is the expected result of the erosion and deposition process without any spatial correlation between cells in the model. This finding complements the results obtained by Larsen et al. [18], in which a differential rate of erosion vs. deposition in the sediment balance is not sufficient to produce stable ridge and slough patterns.

When lateral vegetation growth is considered ($d_{LG}>0$), the ridges and sloughs become thicker in the x-direction. In the variograms shown in Fig. 10, the wavelength in the x-direction (thickness of ridges and sloughs) is similar for lateral growth distances of 1 m, 0.5 m and 0.25 m, so the lateral vegetation growth of the pattern is relatively insensitive to the distance in this range. The wavelength in the y-direction (length of ridges and sloughs) increases with increasing lateral vegetation growth distance. This result can be explained since a larger lateral vegetation growth distance causes increasing sediments being produced and increasing deposition rates in ridge due to a larger flow resistance; this results in an overall larger amount of sediments being deposited in ridge areas generated by an increased lateral growth distance. In slough areas, a larger lateral vegetation growth distance will yield larger flow velocities to satisfy continuity; this will increase erosion rates and enhance the development of slough areas.

Table 2
List of parameters used in model simulations.

Model parameter	Value	Source and notes
Hydraulic conductivity (K)	1.0 [m/s]	[17]
Manning's coefficient (n)	$0.2<n<0.4$	[17,36]
Marsh soil porosity (ϕ)	0.87	Estimated using a bulk density of 200 kg/m^3 [28] and a mean particle density of 1550 kg/m^3 [1]
Brooks and Corey exponent (m)	1.0	[17]
Van Genuchten parameters (α, β)	2.5 m^{-1}, 1.4	[17]
Above ground litter production rate (ε_{prod})	$0.7<\varepsilon_{prod}<2.1$ [g/m^2/day]	[10]
Ratio of below ground to above ground production (f_{BA})	1.0 (base case)	Varied in model simulations
Settling Velocity (v_S)	19 [m/day]	[17]
Resuspension rate at zero water velocity (ε_{res})	16 [g/m^2/day]	[17], fit to data in [19]
Erosion factor (F_E)	0.013 [g/m^2/day]	[17], fit to data in [19]
Initial organic mass fraction (f_O)	0.66	[28]
Initial inorganic mass fraction (f_I)	0.34	$f_I=1-f_O$
Bulk density of particles (ρ_O, ρ_I)	166 [kg/m^3] (organic); 330 [kg/m^3] (inorganic)	[17]
Anaerobic Decomposition Rate (r_{dec})	Anaerobic 0.01 [year^{-1}]; aerobic 0.03 [year^{-1}]	[6]
Ratio of aerobic to anaerobic decomposition rate	3.0	[7]
Grid spacing	0.5 [m] (base case)	Varied in model simulations
Lateral growth parameter (d_{LG})	1.0 [m] (base case)	Varied in model simulations

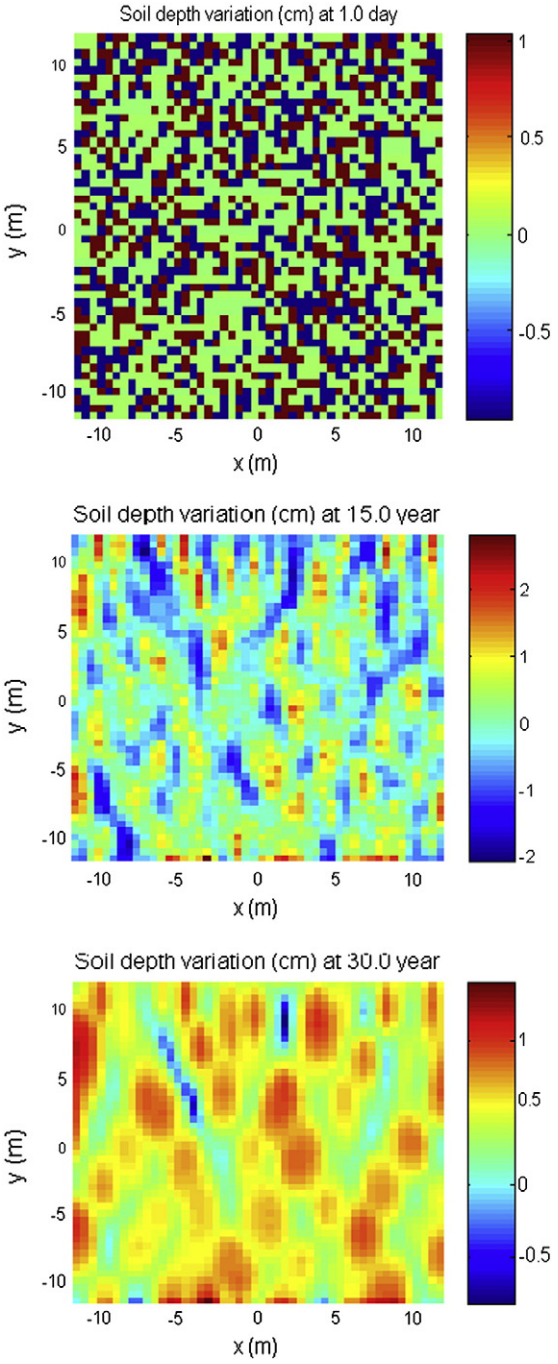

Fig. 6. Development of the ridge and slough pattern for the base case simulation. The plots correspond to soil depth values for simulation times of 1 day (top), 15 years (middle) and 30 years (bottom). Water flows in *y*-direction from the top to the bottom.

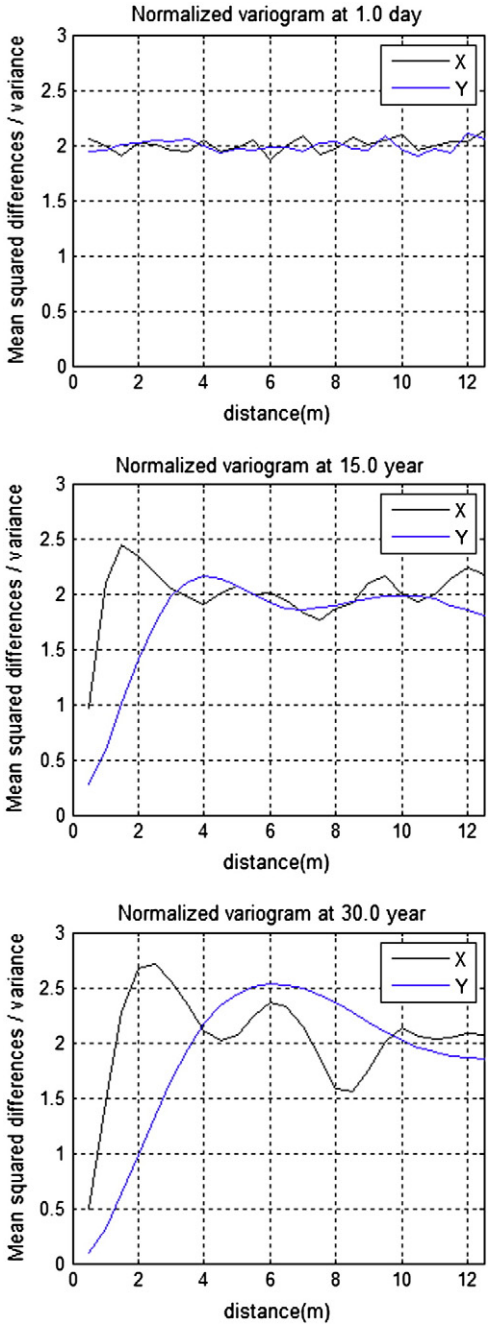

Fig. 7. Variogram of the ridge and slough pattern for the base case simulations shown in Fig. 6. The plots correspond to soil depth differences for simulation times of 1 day (top), 15 years (middle) and 30 years (bottom).

The influence of the lateral vegetation growth distance on the evolution of the pattern is further illustrated in Fig. 11. Essentially, a larger lateral vegetation growth distance results in slower dynamics, i.e., longer "equilibration" times for the pattern since "true" (wider and longer) ridges and sloughs necessarily take longer to develop. Overall, this is an interesting result: the ability of ridges and sloughs to expand laterally not only controls the width of the pattern, but also the length and the characteristic time of development of the pattern. This poses the need to study in more detail the mechanism(s) resulting in lateral growth of ridges and sloughs, as they appear to be a major controlling factor in the development of the pattern in space and over time. The results of this work suggest that the ridge and slough pattern formation occurs as a result of vegetation's ability to grow laterally by production, enhancing sediment deposition in ridge areas, and balanced by increased sediment erosion in slough areas to satisfy continuity.

The effect of biomass production below the ground is shown in Fig. 12. A case without below ground production was considered and compared to the base case (which has equal rates of biomass production above and below ground). The below ground production allocates the mass directly into the soil layer, while the above ground production is applied as the suspended particles in surface water that are transported before reaching the soil. The inclusion of the below ground biomass in the base case enhances the development of the ridge and slough pattern; more production, particularly on the ground, accelerates ridge formation (width and length) and lateral

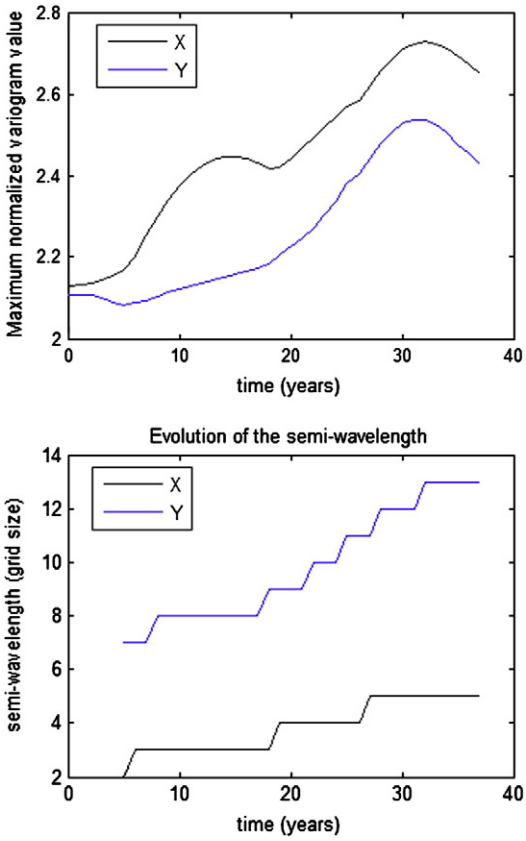

Fig. 8. Evolution of the first maximum value of the variogram (top) and the semi-wavelength of the pattern (bottom) for the base case simulation.

growth of ridges enhances erosion from slough areas, further developing the pattern.

A case with a grid size of 5 m was considered; the results are presented in Fig. 13. The result is the lack of resolution in the pattern shape relative to the base case, which has a grid spacing of 0.5 m. The relation between the maximum grid size and the lateral vegetation growth distance is illustrated in Fig. 14, showing the dependency of the semi-wavelength computed after 20 simulated years and the relative lateral vegetation growth distance. This graph includes all the simulated cases presented in the results above: the base case, the three cases varying the lateral vegetation growth distance, and the cases varying the below ground production and the grid size. These results suggest that the grid cell size in the model should be no greater than half of the lateral vegetation growth distance in order to obtain patterns independent of the model's grid discretization; the base case satisfies this condition, as it has a lateral growth distance of 1 m, and a numerical grid cell size of 0.5 m.

6. Limitations of the approach

It is important to recognize the limitations of the modeling approach developed in this work, with particular respect to the applicability of the results in actual field cases of spatiotemporal patterning of water, sediments and vegetation in wetlands. The model formulation presented in the set of governing equations involves a series of assumptions that although have been justified on a theoretical basis, need to be explored further in developing more realistic applications to actual field cases of pattern formation, maintenance, vulnerability and resilience.

A more detailed formulation of the integrated surface water–groundwater coupled interaction, with particular regard to recharge/discharge exchanges is needed. Groundwater recharge, for instance, is

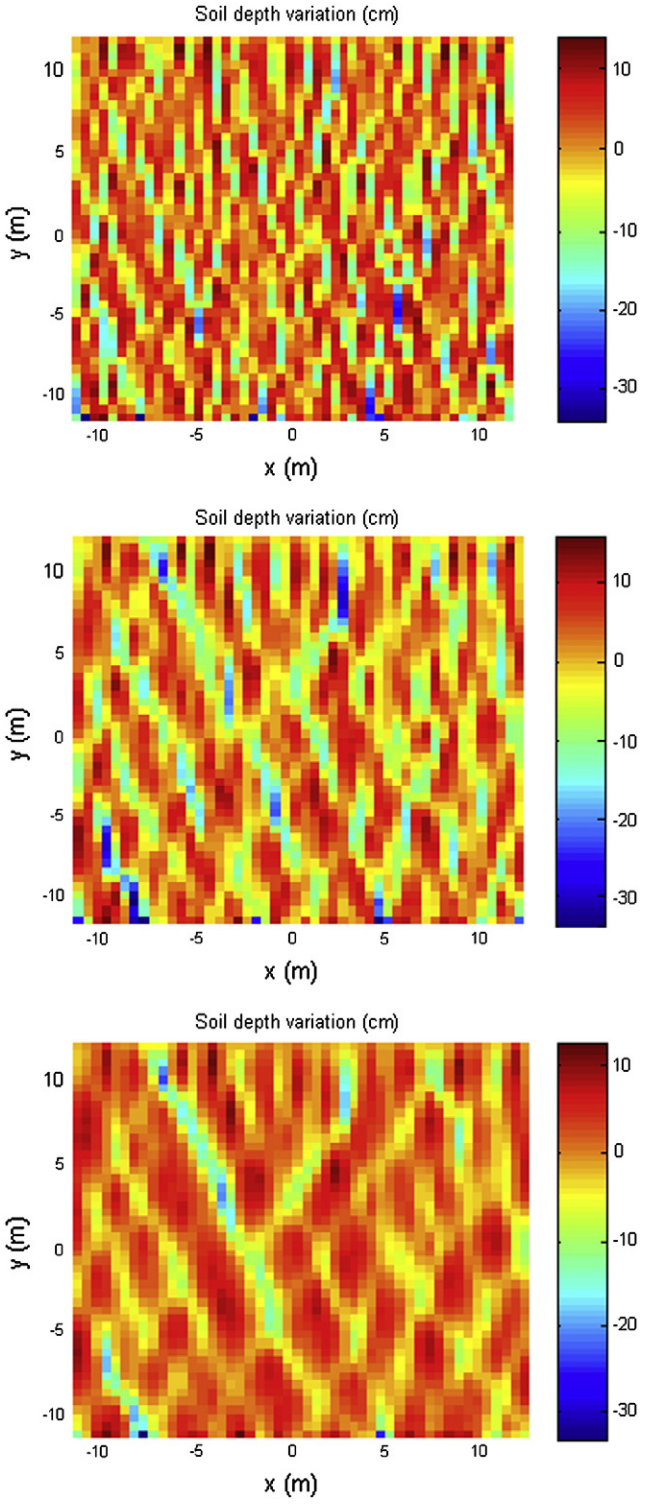

Fig. 9. Development of the ridge and slough pattern with respect to lateral growth distance. The plots correspond to distances of $d_{LG}=0$ (top), $d_{LG}=0.25$ m (middle) and $d_{LG}=0.5$ m (bottom).

not easy to measure directly and estimates of its value are prone to large errors. The most significant and common type of error is found in the conceptual modeling stage; this arises when too many simplifying assumptions are made, such as in this case. We have compared the modeling results in this work with existing (and widely tested) numerical modeling tools Mike-SHE and MODHMS and have found the accuracy and stability of our solver's calculations to be acceptable. However, run times in our simple solver need to be increased

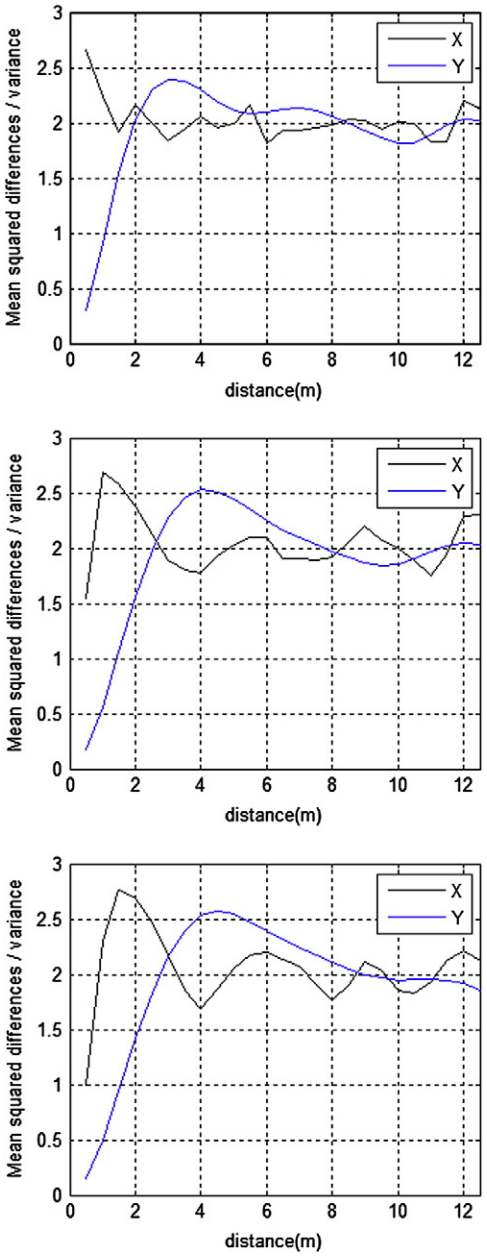

Fig. 10. Variograms of the ridge and slough pattern with respect to lateral growth distance shown in Fig. 9. The plots correspond to distances of $d_{LG}=0$ (top), $d_{LG}=0.25$ m (middle) and $d_{LG}=0.5$ m (bottom).

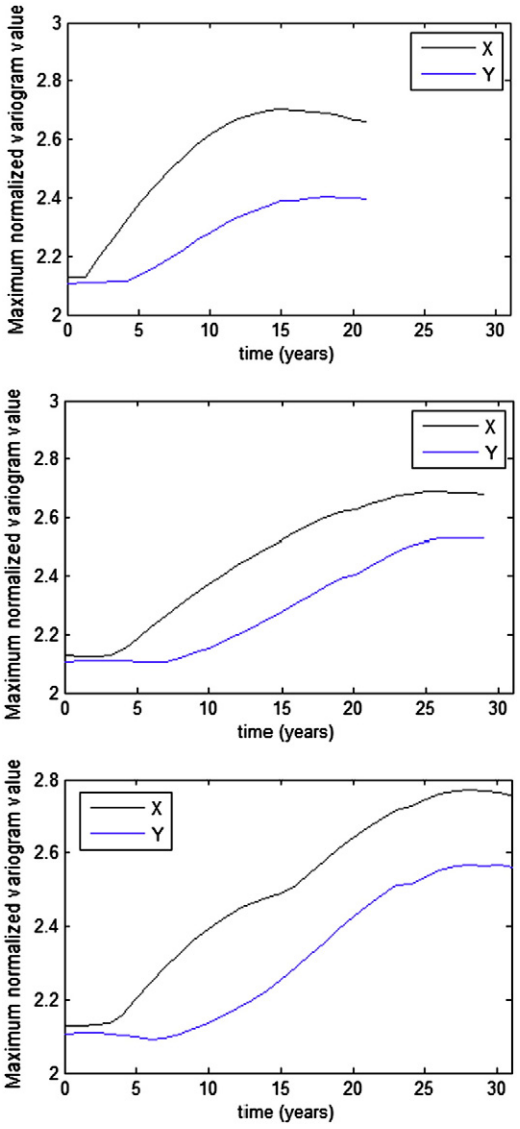

Fig. 11. Evolution of the first maximum value of the variogram of the ridge and slough pattern with respect to lateral growth distance shown in Fig. 10. The plots correspond to distances of $d_{LG}=0$ (top), $d_{LG}=0.25$ m (middle) and $d_{LG}=0.5$ m (bottom).

significantly for our numerical model to be used in practical applications. This is an area in which we have ongoing research efforts.

The processes we are simulating are non-linear in time and space, driven by variations of inputs and properties of soils, sediments and vegetation. For future studies, an error analysis can show which variables in an equation lead to the highest errors, and special effort can be concentrated on obtaining the most accurate estimates for these model parameters. Recognizing that sufficient data with temporal and spatial resolution rarely exists in real wetland application cases (because of difficulty of access and other factors), further efforts should be directed to utilize more than one method of estimation to provide an independent check of model parameter values that can be used for predictive modeling purposes. Also, techniques to analyze the uncertainty of model results will aid in assessing the reliability of these for predictive, management and decision-making purposes.

In spite of its limitations, the modeling approach presented here produces results for the development of ridge and slough patterns that are similar to those observed in the Everglades wetland. The results of Larsen et al. [18], using a different model formulation find that the development and stability of the ridge and slough pattern needs to include phenomena beyond sediment erosion and deposition. The agreement between these disparate methods is important because it provides an independent test of these hypotheses, and moves us closer to practically applicable modeling formulations and tools beyond that developed in this article.

7. Summary

In this investigation, a numerical model of water flow, sediment transport, vegetation litter production, and differential soil accretion is developed and applied to the ridge and slough landscape in the Everglades wetland. This model is used to explore whether observed landscape features and long term stability of the ridge and slough landscape can be explained through this class of feedback processes.

The spatial structure of the simulated ridge and slough patterns is explored through the calculated variogram of the soil depth in the

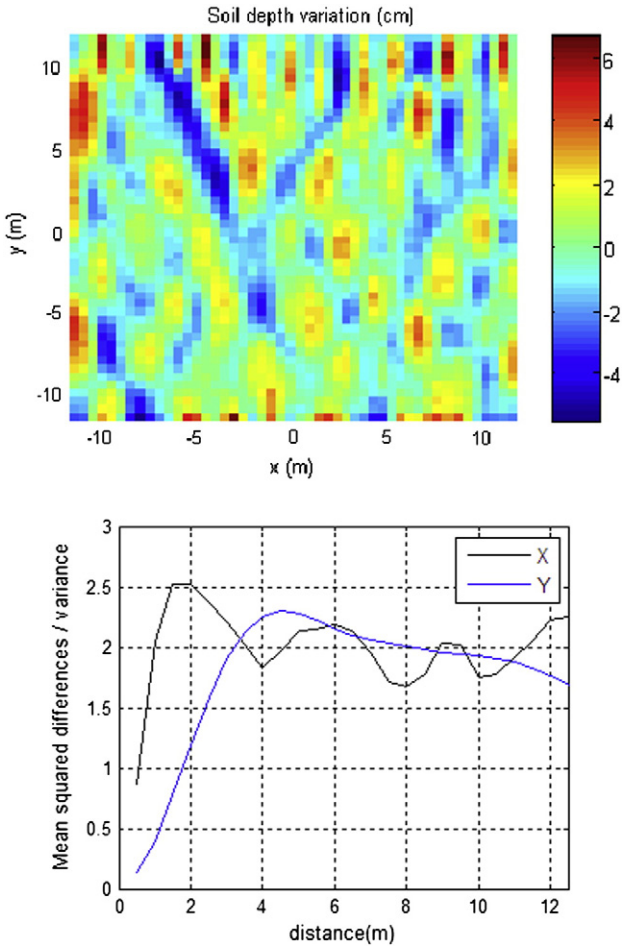

Fig. 12. Development of the ridge and slough pattern and variogram for a case with zero below ground production, i.e. $f_{BA} = 0$ (simulation time is 30 years).

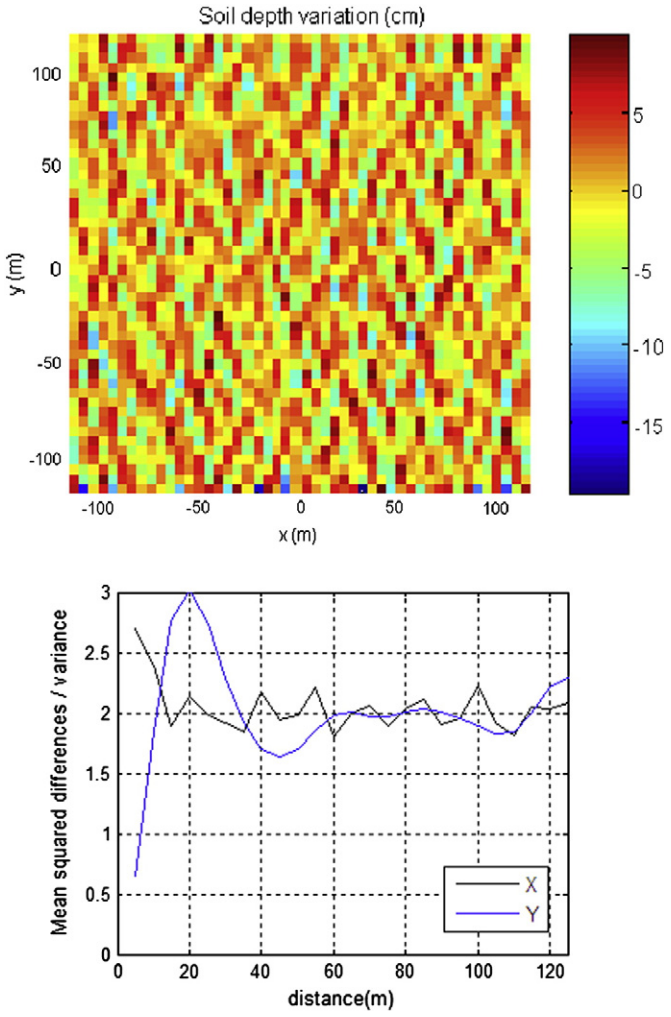

Fig. 13. Development of the ridge and slough pattern and variogram for a case with a numerical grid spacing of 5 m (simulation time is 30 years).

directions along and transverse to flow. The pattern is revealed as a succession of maximum and minimum values in the variogram. The more organized the pattern becomes, the higher the difference between minimum and maximum values (pattern contrast). The model simulations show how the spatial pattern self-organizes over time with the generation of ridges and sloughs driven by differences in litter production and decomposition rates, sediment deposition and erosion, and by the lateral growth of the vegetation.

The model was parameterized with values that are representative of the Everglades wetland in the southern portion of the Florida peninsula in the USA. Model simulation sensitivity was tested with respect to numerical grid size, lateral vegetation growth parameter and rate of below ground production by vegetation. The characteristic wavelengths of ridges and sloughs in the directions along and perpendicular to flow that are simulated with this model are consistent with observed patterns in the field. Also, the simulated elevation differences between the ridges and sloughs are those typically found in the field. The width of ridges and sloughs was found to be controlled by the lateral vegetation growth distance parameter; this complements earlier modeling results in which a differential peat accretion mechanism alone was not found to reproduce observed ridge and slough widths. The sediment transport mechanism alone without inducing a lateral vegetation growth distance was also unable to reproduce ridge and slough patterning.

The results of this work suggest that the ridge and slough pattern formation occurs as a result of vegetation's ability to grow laterally, enhancing sediment deposition in ridge areas, and balanced by increased sediment erosion in slough areas to satisfy flow continuity. The interplay between sediment transport (erosion and deposition), flow and vegetation and soil processes needs to be explored further through detailed field experiments, and use a model formulation such as the one developed in this work to guide data collection and interpretation. This should be one of the focus areas of future investigations of pattern formation and stability in ridge and slough areas.

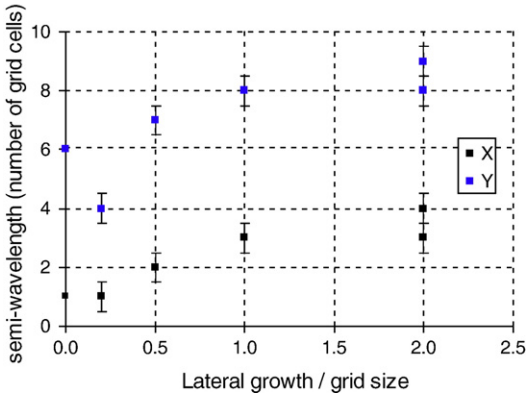

Fig. 14. Dependency of the maximum variogram value (semi-wavelength) computed after 20 simulated years on the relative lateral propagation distance.

Results and insights gained from the conceptual and numerical models presented in this work provide an improved mechanistic understanding of how the landscape may have formed, persisted throughout time, and degraded by changes in water management that resulted from increasing human activity in this wetland over the past decades. This effort is a step further towards a framework for future modeling and data collection research intended to improve management and decision making in ecosystem restoration efforts.

Acknowledgments

Research funding from the National Park Service—Everglades National Park supported the research by M. Lago. An Everglades Fellowship supported the research of M. Mahmoudi. Miralles-Wilhelm was partially supported by a NSF Biocomplexity Award (grant EAR-0608445) as well as the NASA-*WaterSCAPES* (Science of Coupled Aquatic Processes in Ecosystems from Space) University Research Center (grant NNX08BA43A). We thank Michael Ross and Pablo Ruiz of FIU for assistance in developing the vegetation and soil modeling parameters.

References

[1] Bazante J, Jacobi G, Solo-Gabriele HM, Reed D, Mitchell-Bruker S, Childers DL, et al. Hydrologic measurements and implications for tree island formation within Everglades National Park. J Hydrol 2006;329:606–19.
[2] Belyea LR, Lancaster J. Inferring landscape dynamics of bog pools from scaling relationships and spatial patterns. J Ecol 2002;90:223–34.
[3] Couwenberg J. A simulation model of mire patterning: revisited. Ecography 2005;28:653–61.
[4] Couwenberg J, Joosten H. Self-organization in raised bog patterning: the origin of microtope zonation and mesotope diversity. J Ecol 2005;93:1238–48.
[5] Crisfield E, McVoy C. Role of flow-related processes in maintaining the ridge and slough landscape. Joint Conference on the Science and Restoration of the Greater Everglades and Florida Bay Ecosystem, Palm Harbor, FL; 2004.
[6] Davis SM. Growth, decomposition, and nutrient retention of *Cladium jamaicense* Crantz and *Typha domingensis* Pers. in the Florida Everglades. Aquat Bot 1991;40:203–24.
[7] DeBusk WF, Reddy KR. Turnover of detrital organic carbon in a nutrient-impacted Everglades marsh. Soil Sci Soc Am J 1998;62:1460–8.
[8] Douglas MS. The Everglades river of grass. Sarasota FL: Pineapple Press; 1947.
[9] Ellery WN, McCarthy TS, Smith ND. Vegetation, hydrology, and sedimentation patterns on the major distributary system of the Okavango Fan, Botswana. Wetlands 2003;23:357–75.
[10] Ewe SML, Gaiser EE, Childers DL, Iwaniec D, Rivera-Monroy VH, Twilley RR. Spatial and temporal patterns of aboveground net primary productivity (ANPP) along two freshwater–estuarine transects in the Florida Coastal Everglades. Hydrobiologia 2006;569:459–74.
[11] Foster DR, King GA, Glaser PH, Wright HE. Origin of string patterns in boreal peatlands. Nature 1983;306:256–8.
[12] Gumbricht T, McCarthy J, McCarthy TS. Channels, wetlands, and islands in the Okavango Delta, Botswana, and their relation to hydrological and sedimentological processes. Earth Surf Process Land 2004;29:15–29.
[13] Istanbulluoglu E, Bras RL. On the dynamics of soil moisture, vegetation and erosion: implications of climate variability and change. Water Resour Res 2006;42:W06418, doi:10.1029/2005WR004113.
[14] Klausmeier CA. Regular and irregular patterns in semiarid vegetation. Science 1999;284:1826–8.
[15] Lal AMW. Performance comparison of overland flow algorithms. J Hydraul Eng 1998;124:342–9.
[16] Lal AMW. Numerical errors in groundwater and overland flow models. Water Resour Res 2000;36:1237–47.
[17] Lago, M.E., 2009, A model to describe spatial and temporal variation of phosphorous cycling in tree islands of Shark River Slough in the Everglades, Ph. D. Thesis, University of Miami.
[18] Larsen LG, Harvey JW, Crimaldi JP. A delicate balance: ecohydrological feedbacks governing landscape morphology in a lotic peatland. Ecol Monogr 2007;77(4):591–614.
[19] Leonard L, Croft A, Childers D, Mitchell-Bruker S, Solo-Gabriele H, Ross M. Characteristics of surface-water flows in the ridge and slough landscape of Everglades National Park: implications for particulate transport. Hydrobiologia 2006;569:5–22.
[20] Lindsay RA, Rigall J, Burd F. The use of small-scale surface patterns in the classification of British peatlands. Aquilo Ser Bot 1985;21:69–79.
[21] Moreira MZ, Sternberg LSL, Martinelli LA, Victoria RL, Barboza EM, Bonates LCM, et al. Contribution of transpiration to forest ambient vapor based on isotopic measurements. Glob Change Biol 1997;3:439–50.
[22] Ogden JC. Everglades ridge and slough conceptual ecological model. Wetlands 2005;25:810–20.
[23] Oyama MD, Nobre CA. A new climate-vegetation equilibrium state for tropical South America. Geophys Res Lett 2003;30:51–5.
[24] Porporato A, Laio F, Ridolfi L, Rodriguez-Iturbe I. Plants in water-controlled ecosystems: active role in hydrologic processes and response to water stress III: vegetation water stress. Adv Water Res 2001;24:725–44.
[25] Querejeta JI, Estrada-Medina H, Allen MF, Jimenez-Osornio JJ. Water source partitioning among trees growing on shallow karst soils in a seasonally dry tropical climate. Oecologia 2007;152:26–36.
[26] Ridolfi L, D'Odorico P, Porporato A, Rodriguez-Iturbe I. Duration and frequency of water stress in vegetation: an analytical model. Water Resour Res 2000;36(8):2297–307.
[27] Rietkerk M, Dekker SC, Wassen MJ, Verkroost AWM, Bierkens MFP. A putative mechanism for bog patterning. Am Nat 2004;163:699–708.
[28] Ross MS, Mitchell-Bruker S, Sah JP, Stothoff S, Ruiz PL, Reed DL, et al. Interaction of hydrology and nutrient limitation in the Ridge and Slough landscape of the southern Everglades. Hydrobiologia 2006;569:37–59.
[29] Sakaguchi Y. On the genesis of banks and hollows in peat bogs: an explanation by a thatch line theory. Bull Dept Geogr Univ Tokyo 1980;12:35–58.
[30] San Jose JJ, Meirelles ML, Bracho R, Nikonovan N. A comparative analysis of the flooding and fire effects on the energy exchange in a wetland community (Morichal) of the Orinoco Llanos. J Hydrol 2001;242:228–54.
[31] Science Coordination Team. The role of flow in the Everglades ridge and slough landscape. South Florida Ecosystem Restoration Working Group, U.S. Geological Survey, Washington, D.C., USA; 2003. Available online: http://sofia.usgs.gov/publications/papers/sct_flows/i.
[32] Silva MPD, Mauro R, Mourao G, Coutinho M. Distribuicao e quantificacao de classes de vegetacao do Pantanal atraves de levantamento aereo. Rev Bras Bot 1999;23.
[33] Sternberg LSL, Moreira MZ, Nepstad DC. Uptake of water by lateral roots in an Amazonian tropical forest. Plant Soil 2002;238:151–8.
[34] Swanson DK, Grigal DF. A simulation model of mire patterning. Oikos 1988;53:309–14.
[35] Van Genuchten MTh, Leij FJ, Yates SR. The RETC code for quantifying the hydraulic functions of unsaturated soils, EPA/600/2-91/065; 1991. 93 pp.
[36] Van Wijk MT, Rodriguez-Iturbe I. Tree-grass competition in space and time: insights from a simple cellular automata model based on ecohydrological dynamics. Water Resour Res 2002;38:1179–93.
[37] Wdowinski S, Amelung F, Miralles-Wilhelm F, Dixon TH, Carande R. Space-based measurements of sheet-flow characteristics in the Everglades wetland, Florida. Geophys Res Lett 2004;31:L15503, doi:10.1029/2004GL020383.
[38] Davis SM. Phosphorus inputs and vegetation sensitivity in the everglades. In: Davis SM, Ogden JC, editors. Everglades: The Ecosystem and Its Restoration. Delray Beach: St. Lucie Press; 1994; pp. 357–378.